ADAPTIVE MESH REFINEMENT FOR ELLIPTIC INTERFACE PROBLEMS USING THE NON-CONFORMING IMMERSED FINITE ELEMENT METHOD

CHIN-TIEN WU, ZHILIN LI, AND MING-CHIH LAI

Abstract. In this paper, an adaptive mesh refinement technique is developed and analyzed for the non-conforming immersed finite element (IFE) method proposed in [27]. The IFE method was developed for solving the second order elliptic boundary value problem with interfaces across which the coefficient may be discontinuous. The IFE method was based on a triangulation that does not need to fit the interface. One of the key ideas of IFE method is to modify the basis functions so that the natural jump conditions are satisfied across the interface. The IFE method has shown to be order of $O(h^2)$ and $O(h)$ in L^2 norm and H^1 norm, respectively. In order to develop the adaptive mesh refinement technique, additional priori and posterior error estimations are derived in this paper. Our new a-priori error estimation shows that the generic constant is only linearly proportional to ratio of the diffusion coefficient β^- and β^+, which improves the corresponding result in [27]. We also show that a-posteriori error estimate similar to the one obtained by Bernardi and Verfürth [4] holds for the IFE solutions. Numerical examples support our theoretical results and show that the adaptive mesh refinement strategy is effective for the IFE approximation.

Key Words. interface, immersed finite element, adaptive mesh

1. Introduction

The main purpose of this paper is to develop adaptive mesh refinement techniques for the immersed finite element (IFE) method proposed in [27]. Along this line, we also discuss a-priori and a-posteriori error estimates for the immersed finite element method. The IFE method was developed for the following interface problem:

$$
\begin{aligned}
-\nabla \cdot (\beta \nabla u) &= f, \ (x,y) \in \Omega \\
u \mid_{\partial \Omega} &= g,
\end{aligned}
\tag{1}
$$

together with the natural jump conditions across the interface $\tilde{\Gamma}$:

$$
[u] \mid_{\tilde{\Gamma}} = 0,
\tag{2}
$$

$$
[\beta u_n] \mid_{\tilde{\Gamma}} = 0.
\tag{3}
$$

Here, $\Omega \subset \mathbb{R}^2$ is a convex polygonal domain, the interface $\tilde{\Gamma}$ is a curve separating Ω into two sub-domains Ω^-, Ω^+ such that $\Omega = \Omega^- \cup \Omega^+ \cup \tilde{\Gamma}$, and the coefficient $\beta(x, y)$ is a piecewise continuous function

$$\beta(x, y) = \begin{cases} \beta^-(x, y), & (x, y) \in \Omega^-, \\ \beta^+(x, y), & (x, y) \in \Omega^+, \end{cases}$$

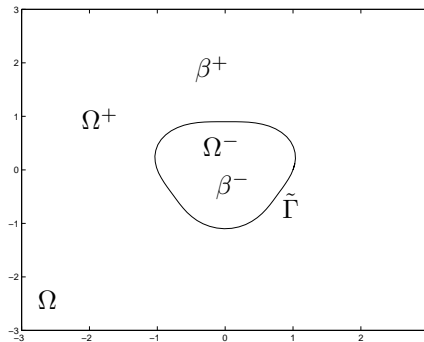see the diagram in Fig. 1 for an illustration.

FIGURE 1. A rectangular domain $\Omega = \Omega^+ \cup \Omega^-$ with an immersed interface $\tilde{\Gamma}$. The coefficients $\beta(\mathbf{x})$ may have a jump across the interface.

The interface problem considered here appears in many engineering and science applications. The immersed finite element (IFE) space was first introduced in [27], in which some preliminary analysis and numerical results are reported. The new IFE method has been developed for non-homogeneous jump conditions (with nonzero right hands of (2) and (3)) in [25]. Some related work can be found in [19, 20, 24, 28].

The basic idea of the immersed finite elements is to form a partition $\Im_h$ independent of interface $\tilde{\Gamma}$ so that partitions with simple regular structures can be used to solve an interface problem with a rather complicated or varying interface. Obviously, triangles in a partition can be separated into two classes:

• Non-interface triangles: The interface $\tilde{\Gamma}$ either does not intersect with this triangle, or it intersects with this triangle but does not separate its interior into two nontrivial subsets.

• Interface triangles: The interface $\tilde{\Gamma}$ cuts through its interior.

In a non-interface triangle, the standard linear polynomials is employed as local basis functions. However, in an interface triangle, a piecewise linear polynomial is defined in the two subsets formed by the interface in a way that the functions satisfy the natural jump conditions (either exactly or approximately) on the interface and retain specified values at the vertices of the interface triangle. The immersed finite element space defined over the whole domain Ω can then be constructed through the standard finite element assembling procedure. We refer the readers to [9–12, 15, 18, 23, 26] for more background materials about immersed interface and immersed finite element methods as well as their applications.

Without loss of generality, we assume that the triangles in the partition have the following features:

(H_1): If $\tilde{\Gamma}$ meets one edge of a triangle at more than two points, then the edge is part of $\tilde{\Gamma}$.

(H_2): If $\tilde{\Gamma}$ meets a triangle at two points, then these two points must be on different edges for this triangle.

In order to obtain error estimates, we assume that the underlying mesh is fine enough such that the interface can be approximated by a line segment with a small perturbation in a magnitude of $O(h^2)$. Furthermore, the source function f and the interface $\tilde{\Gamma}$ are assumed to be smooth enough such that the weak solution of the problem (1) can be approximated by a piecewise C^2 function. These requirements lead to our third hypothesis:

(H_3): The segment of the interface $\tilde{\Gamma}$ in a triangle $T \in \Im_h$ is defined by a piecewise C^2 function and the function space $C^2(T)$ is dense in $H^2(T)$.

It is well known that the standard finite element method (FE) with linear finite elements can be used to solve such elliptic interface problems, see [3, 5, 6] and the references therein. However, in order to achieve the optimal $O(h^2)$ accuracy in the numerical solutions, an interface fitted grid is needed. In applications with nontrivial interfaces or the time-varying interfaces, this restriction prevents the Galerkin method with linear finite elements from working efficiently since mesh moving or re-meshing is required. On the other hand, although the mesh moving and re-meshing may produce extra technical difficulties and computation overhead for the standard FE method, the standard FE method has a great advantage on increasing the accuracy of the numerical solutions at low cost through the adaptive mesh refinement process. In the adaptive mesh refinement process, first an error indicator η_T used to pin point the locations with large error is computed on each element in a given triangulation. Second, the elements in which the error indicator has large value are marked for refinement according to a given marking strategy. A heuristic marking strategy is the maximum marking strategy where an element T^* will be marked for refinement if $\eta_{T^*} > \theta \max_{T \in \Im_h} \eta_T$, with a prescribed threshold $0 \leq \theta \leq 1$. Some other marking strategies can also be seen in [14]. Finally, the marked triangles are divided into sub-triangles by rules such as the regular refinement algorithm or the longest side bisection algorithm [16, 17]. An approximate solution is then computed on the refined mesh. The above procedure can be repeatedly applied until the accuracy of the approximated solution is satisfied. The theoretical foundation of the mesh refinement strategy is based on the a-posteriori error estimation proposed by Babuška and Rheinboldt [1] and further developed by many researchers such as Zienkiewicz [29], Bank and Weiser [2], and Verfürth [21, 22]. The convergence of the adaptive mesh refinement process has been shown by Morin, Nochetto and Siebert [13].

It has been shown that the IFE interpolation errors on a uniform fixed (such as Cartesian) partition is of the order of $O(h)$ in the H^1 norm and of the order of $O(h^2)$ in the L^∞ and L^2 norms under the hypothesis (H_1), (H_2) and (H_3) [28]. In this work, we obtain the same order of the error estimations and further show that the generic constants in these estimations are linearly proportional to the ratio $\max\{\rho, 1/\rho\}$ of the diffusion coefficients, here $\rho = \beta^-/\beta^+$. The a-posteriori estimations of the finite element solutions mentioned above are obtained mostly on fitted grids. Recently, A. Hansbo and P. Hansbo propose an unfitted finite element method for the elliptic interface problem. The same order of a-priori error estimations is obtained and an a-posteriori estimator is proposed [8]. Here, we also

derive an a-posteriori error estimation for the IFE method based on the method-
ology developed by Verfürth [4]. Our numerical results support the effectiveness of
the proposed a-posteriori error estimation.

This paper is organized as follows. In section 2, we show the existence and
uniqueness of the element IFE basis function and derive some auxiliary inequali-
ties that are needed for the error estimation in section 3. We derive the a-priori
error estimations and the a-posteriori error estimation in section 3 and present our
numerical results in section 4. Finally, we draw our conclusions in section 5.

2. Review of the immersed finite element space

First we present a brief review of the immersed finite element space and the
construction of the basis functions.

Given a regular mesh $\Im_h$ on the domain Ω, let T be an interface triangle in
$\Im_h$ with vertices A, B and C where the interface passes through the interior of
T and intersect with the edges of T at points D and E. Let $\tilde{\Gamma}_T = \tilde{\Gamma} \cap T$. In
the immersed finite element method, the interface $\tilde{\Gamma}_T$ is commonly approximated
by the line segment $\overline{DE}$, denoted by Γ_T. The formulation of the immersed finite
element method follows the idea that similar to the Hsieh-Clough-Tocher macro
element [7] in which the piecewise polynomial in each element is required to satisfy
certain constrains to ensure the C^1-continuity on the whole domain. The immersed
finite element space on a triangle T, denoted by $S_h^I(T)$, is the linear space of all
piecewise linear functions that satisfy the continuity condition $[\phi]_{\Gamma_T} = 0$ and the
homogeneous flux jump condition $[\beta \partial_n \phi]_{\Gamma_T} = 0$ on the approximate interface Γ_T.
Assume the element basis functions on the reference triangle have the following
form:

$$\phi^+ = a_0 + a_1 x + a_2 y \ \text{ for } (x, y) \in T^+$$
$$\phi^- = b_0 + b_1 x + b_2 y \ \text{ for } (x, y) \in T^-.$$

It has been shown that the coefficients a_i and b_i, $i = 1 \cdots 3$, can be determined
uniquely. In [27], the continuity condition $[\phi]_{\Gamma_T} = 0$ is satisfied by enforcing the
continuity on the intersection points D and E, i.e., $\phi^+(D) = \phi^-(D)$ and $\phi^+(E) =
\phi^-(E)$. In this work, we replace the condition $\phi^+(E) = \phi^-(E)$ by $\vec{t} \cdot \nabla \phi^+ =
\vec{t} \cdot \nabla \phi^-$, here $\vec{t}$ is the unit tangent of the approximated interface Γ_T. The existence
and uniqueness of the immersed finite element basis functions are reassured in the
following theorem. The interpolation errors in the L^∞, L^2 and H^1 norms will be
estimated in the next section.

Theorem 2.1. *Let T denote a triangle with vertices (x_i, y_i), $i = 1 \cdots 3$ in a
given uniform mesh, the associated IFE basis functions $\phi \in S_h^I(T)$ consisting of
ϕ^+ and ϕ^- on the reference triangle are uniquely determined by the nodal values
$\phi(x_i, y_i)$, $i = 1 \cdots 3$.*

Proof: Let Φ be the affine transformation that maps the reference triangle to
the triangle T via $\Phi(0, 0) = (x_1, y_1)$, $\Phi(1, 0) = (x_2, y_2)$ and $\Phi(0, 1) = (x_3, y_3)$. Let
$\phi(x_i, y_i) = \phi_i$, $i = 1 \cdots 3$. From the nodal values and the continuity at node D, we
have

$$(4) \qquad \phi_3 = \phi^+(0, 1) = a_0 + a_2 \Rightarrow a_0 = \phi_3 - a_2$$
$$(5) \qquad \phi_1 = \phi^-(0, 0) = b_0$$
$$(6) \qquad \phi_2 = \phi^-(1, 0) = b_0 + b_1 \Rightarrow b_1 = \phi_2 - \phi_1$$
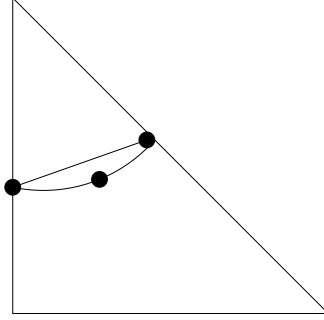$$(7) \qquad a_0 + a_2 \hat{y}_1 = b_0 + b_2 \hat{y}_1.$$

FIGURE 2. A typical triangle element with an interface cutting through. The arc DME is part of the interface curve $\tilde{\Gamma}$ which is approximated by the line segment $\overline{DE}$. In this picture, T is the triangle $\triangle ABC$, $T^+ = \triangle ADE$, $T^- = T - T^+$, and T^* is the region enclosed by the $\overline{DE}$ and $\tilde{\Gamma}$.

Plugging equations (4) and (5) into equation (7) implies

$$(8) \qquad (-1 + \hat{y}_1)a_2 - \hat{y}_1 b_2 = \phi_1 - \phi_3.$$

Moreover, from the flux continuity condition and the continuity of the solution along the tangential direction of the interface, we have

$$(9) \qquad \begin{cases} \vec{n}(\Phi^{-1})^T \nabla \phi^+ = \rho \vec{n}(\Phi^{-1})^T \nabla \phi^- \\ \vec{t}(\Phi^{-1})^T \nabla \phi^+ = \vec{t}(\Phi^{-1})^T \nabla \phi^-, \end{cases}$$

where $n = (n_1, n_2)$ and $t = (-n_2, n_1)$ are the normal and tangent vectors of the interface respectively, and $\rho = \beta^- / \beta^+$. Let $(m_1, m_2) = \vec{n}(\Phi^{-1})^T$ and $(m_3, m_4) = \vec{t}(\Phi^{-1})^T$. The two equations in (9) can be rewritten as following:

$$(10) \qquad m_1 a_1 + m_2 a_2 - \rho m_2 b_2 = -\rho m_1 \phi_1 + \rho m_1 \phi_2$$

$$(11) \qquad m_3 a_1 + m_4 a_2 = m_3(\phi_2 - \phi_1) + m_4 b_2.$$

Plugging (8) into (10) and (11) and writing the resulted equations in the matrix form, we have

$$(12) \qquad \begin{aligned} & \begin{bmatrix} m_1 \hat{y}_1 & m_2(\hat{y}_1 + \rho(1 - \hat{y}_1)) \\ m_3 \hat{y}_1 & m_4 \end{bmatrix} \begin{bmatrix} a_1 \\ a_2 \end{bmatrix} \\ & = \begin{bmatrix} (-\rho m_2 - \rho m_1 \hat{y}_1) & \rho m_1 \hat{y}_1 & \rho m_2 \\ -m_4 - m_3 \hat{y}_1 & m_3 \hat{y}_1 & m_4 \end{bmatrix} \begin{bmatrix} \phi_1 \\ \phi_2 \\ \phi_3 \end{bmatrix} \\ & = \begin{bmatrix} \rho m_1 \hat{y}_1 & \rho m_2 \\ m_3 \hat{y}_1 & m_4 \end{bmatrix} \begin{bmatrix} \phi_2 - \phi_1 \\ \phi_3 - \phi_1 \end{bmatrix}. \end{aligned}$$

To prove the theorem, we only need to show the metric

$$A = \begin{bmatrix} m_1 \hat{y}_1 & m_2(\hat{y}_1 + \rho(1 - \hat{y}_1)) \\ m_3 \hat{y}_1 & m_4 \end{bmatrix}$$

is non-singular. Let $\rho^* = \hat{y}_1 + \rho(1 - \hat{y}_1)$. We can see clearly that $\rho^* \geq 1$ when $\rho \geq 1$ and $0 \leq \rho^* \leq 1$ when $\rho \leq 1$. Since $m_1 m_4 - m_2 m_3 = det(\Phi) > 0$, $m_2 m_3 < 0$ and

$m_1 m_4 > 0$, we have

(13) $det(A) = \hat{y}_1((m_1 m_4 - m_2 m_3) - (\rho^* - 1)m_2 m_3) > 0$, if $\rho \geq 1$

and

(14) $det(A) = m_1 m_4 (1 - \rho^*)\hat{y}_1 + \rho^* \hat{y}_1 (m_1 m_4 - m_2 m_3) > 0$, if $0 < \rho < 1$.

Now from (13) and (14), we can conclude the matrix A is nonsingular and the theorem holds. $\square$

Remark 2.2. *We can further estimate*

$$
\begin{aligned}
det(A) &= \hat{y}_1(h^{-2} + (\rho^* - 1)n_y^2) = h^{-2}(\hat{y}_1 \rho^*) \\
&= h^{-2}(\hat{y}_1(\hat{y}_1 + \rho(1 - \hat{y}_1))) > \min\{1, \rho\}\,\hat{y}_1 h^{-2}, \quad \text{for } \rho > 1, \text{ and} \\
det(A) &= h^{-2}\hat{y}_1 > \min\{1, \rho\}\,\hat{y}_1 h^{-2}, \quad \text{for } 0 \leq \rho \leq 1,
\end{aligned}
$$

from the equations (13) and (14), respectively. Therefore, the following estimation of $det(A)$ *holds*

(15) $$det(A) \geq \hat{y}_1 h^{-2} \min\{1, \rho\}.$$

Moreover, Let $\Delta\phi_1 = \phi_2 - \phi_1$, $\Delta\phi_2 = \phi_3 - \phi_1$, *and* $B = \begin{bmatrix} \rho m_1 \hat{y}_1 & \rho m_2 \\ m_3 \hat{y}_1 & m_4 \end{bmatrix}$.

The equation (12) implies

(16) $\begin{bmatrix} a_1 - \Delta\phi_1 \\ a_2 - \Delta\phi_2 \end{bmatrix} = A^{-1}(B - A)\begin{bmatrix} \Delta\phi_1 \\ \Delta\phi_2 \end{bmatrix}$

$$= \frac{\hat{y}_1(\rho - 1)}{\det(A)}\begin{bmatrix} m_2 m_4 & m_2 m_4 \\ -\hat{y}_1 m_2 m_3 & -\hat{y}_1 m_2 m_3 \end{bmatrix}\begin{bmatrix} \Delta\phi_1 \\ \Delta\phi_2 \end{bmatrix}.$$

Also, from the equations (6), (8), and (16), we have

(17) $\begin{bmatrix} b_1 - \Delta\phi_1 \\ b_2 - \Delta\phi_2 \end{bmatrix} = \begin{bmatrix} 0 \\ \frac{\hat{y}_1 - 1}{\hat{y}_1}(a_2 - \Delta\phi_2) \end{bmatrix}$

$$= \frac{\hat{y}_1(\hat{y}_1 - 1)(\rho - 1)}{\det(A)}\begin{bmatrix} 0 & 0 \\ -m_2 m_3 & -m_2 m_3 \end{bmatrix}\begin{bmatrix} \Delta\phi_1 \\ \Delta\phi_2 \end{bmatrix}$$

By applying the estimation (15) to the equations (16) and (17), we can easily show that the following inequalities hold:

(18)

$$\left\|\begin{pmatrix} a_2 - \Delta\phi_1 \\ a_3 - \Delta\phi_2 \end{pmatrix}\right\|_\infty \leq c^+ \max\{\rho, \frac{1}{\rho}\}\left\|\begin{pmatrix} \Delta\phi_1 \\ \Delta\phi_2 \end{pmatrix}\right\|_\infty,$$

$$\left\|\begin{pmatrix} b_2 - \Delta\phi_1 \\ b_3 - \Delta\phi_2 \end{pmatrix}\right\|_\infty \leq c^- \max\{\rho, \frac{1}{\rho}\}\left\|\begin{pmatrix} \Delta\phi_1 \\ \Delta\phi_2 \end{pmatrix}\right\|_\infty,$$

where c^+ *and* c^- *are constants independent with* ρ.

3. The priori and posteriori error estimations

In this section, we define the IFE solution of the interface problem (1) and derive the priori and posteriori error estimations of the IFE solution. We first introduce some notations in the following:

- Let $\Im_h$ denote the regular mesh that satisfies the usual admissibility and the shape regularity. Let $\breve{\Im}_h$ be the set of elements intersect with the interface, and $\overset{\circ}{\Im}_h = \Im_h \setminus \breve{\Im}_h$. For $\tau \in \Im_h$, let $\partial\tau$ denote the set of boundary segments of the element τ and $\mathcal{E}_h = \cup_{\tau \in \Im_h}\partial\tau$. Let $\breve{\mathcal{E}}_h$ be the set of edges intersect

with the interface and $\overset{\circ}{\mathcal{E}}_h = \mathcal{E}_h \setminus \breve{\mathcal{E}}_h$. Moreover, N_h = the set of all vertices in $\Im_h$, N_τ = vertices of an element τ and N_e = vertices of an edge $e \in \mathcal{E}_h$. Also, for any element $\tau \in \Im_h$, edge $e \in \mathcal{E}$ and node $z \in N_h$, let

$$\omega_\tau = \bigcup_{\tau' \cap \tau \in \partial\tau} \tau', \quad \tilde{\omega}_\tau = \bigcup_{\tau' \cap \tau \neq \emptyset} \tau', \quad \omega_e = \bigcup_{N_\tau \cap N_e \neq \emptyset'} \tau', \quad \omega_z = \bigcup_{z \in \tau'} \tau'$$

- We denote by H^0 and H^k, the usual Lebesgue L^2-integrable space and the Sobolev spaces equipped with the standard norms $\|f\|_k$ for $f \in H^k$, $k = 0 \cdots 2$. The notations $\|f\|_{k,\Omega_0}$, $k = 0 \cdots 2$, and $\|f\|_{\beta,\Omega_0}$ denote the usual Sobolev norms and the energy norm of f on a sub-domain $\Omega_0 \subset \Omega$. The piecewise linear polynomial space on a sub-domain Ω_0 is denoted by $S_h(\Omega_0)$. The immersed finite element space on the domain Ω, is denoted by $S_h^I(\Omega)$, is defined by $S_h^I(\Omega) = \{\phi \mid \phi|_\tau \in S_h^I(\tau), \text{ for all } \tau \in \Im_h, \text{ and } \phi|_\tau(z) = \phi|_{\tau'}(z), \text{ for } z \in N_\tau \cap N_{\tau'}\}$. The notation $S_{h,0}^I(\Omega)$ denote the subspace in $S_h^I(\Omega)$ with homogeneous boundary condition, $\{\phi \in S_h^I(\Omega) \mid \phi|_{\partial\Omega} = 0\}$.
- For each vertex $z \in N_h$, let φ_z denote the linear nodal basis function. With every element τ and every edge e, we associate the bubble functions $\psi_\tau = 27 \prod_{z \in N_\tau} \varphi_z$ and $\psi_e = 4 \prod_{z \in N_e} \varphi_z$. Let I_n denote the nodal interpolant, π_z denote the L^2 orthogonal projection onto the piecewise linear function space in ω_z, and I_π denote the quasi-interpolant of a function u defined as $I_\pi u = \sum_{z \in \Im_h} (\pi_z u)\varphi_z$.

For any function $\phi \in H^2(\Omega)$, the IFE interpolant of ϕ is denoted by $\phi_I \in S_h^I$ that satisfies $\varphi_z(\phi_I) = \phi(z)$ for all $z \in N_h$. The IFE solution of problem (1) denoted by u_h^I satisfies the standard variation formulation of (1) as following:

$$(\beta\nabla\nu \,,\, \nabla u_h^I) = (\nu \,,\, f), \text{ for all } \nu \in S_{h,0}^I(\Omega),$$

where $(\cdot \,,\, \cdot)$ is the usual inner product in the $H^0(\Omega)$. To derive the a-priori error estimations of $\left\|u - u_h^I\right\|_0$ and $\left\|u - u_h^I\right\|_1$, we need to estimate the interpolation errors of $\phi - \phi_I$ for any $\phi \in H^1(\Omega) \cap C(\Omega)$, here $\phi_I \in S_h^I(T)$ denote the IFE interpolant of ϕ. In the following theorem, we first estimate the errors of $\phi - \phi_I$ and $\nabla\phi - \nabla\phi_I$ in the L^∞ norm.

Theorem 3.1. *Let T be a triangle in a uniform mesh $\Im_h$ and the interface $\tilde{\Gamma}$ satisfies the hypothesis (H1), (H2) and (H3). Let Γ_T denote the line segment that approximates $\tilde{\Gamma}_T$. Let ϕ be an arbitrary function in $C^2(T)$ and $\phi_I \in S_h^I(T)$ be the IFE interpolant of ϕ. The following error estimates hold.*

$$(19) \quad \|\nabla\phi(x,y) - \nabla\phi_I(x,y)\|_{\infty,T} \leq \begin{cases} ch \left\|D^2\phi\right\|_{\infty,T} & \text{when } (x,y) \in \Omega \setminus T^* \\ c \left\|D^2\phi\right\|_{\infty,T} & \text{when } (x,y) \in T^* \end{cases}$$

$$(20) \qquad \|\phi(x,y) - \phi_I(x,y)\|_{\infty,T} \leq ch^2 \left\|D^2\phi\right\|_{\infty,T},$$

where $c = O(\max\{\frac{1}{\rho}, \rho\})$ and T^* is the region enclosed by $\tilde{\Gamma}_T$ and Γ_T.

Proof: First, we estimate the error of $\nabla\phi - \nabla\phi_I$ at element nodal points of the reference triangle in the following: From the Taylor expansion of ϕ, we have

$$(21) \qquad \phi^+(\hat{x}, \hat{y}) = \phi^+(0,1) + \nabla\phi^+(0,1)\begin{bmatrix} \hat{x} \\ \hat{y} - 1 \end{bmatrix} + e_1$$

$$(22) \qquad \phi^-(\hat{x}, \hat{y}) = \phi^-(0,0) + \nabla\phi^-(0,0)\begin{bmatrix} \hat{x} \\ \hat{y} \end{bmatrix} + e_2,$$

where $e_1 \leq (\hat{y}_1 - 1)(\left\|D^2\phi\right\|_\infty (\hat{y}_1 - 1)h^2)$ and $e_2 \leq \hat{y}_1 \left\|D^2\phi\right\|_\infty \hat{y}_1 h^2$, and $|e_2 - e_1| \leq 2\max_{v \in \{|\hat{y}_1|, |\hat{y}_1 - 1|\}}\{v^T \left\|D^2\phi\right\|_\infty v\}h^2$. By imposing the continuity at node D, from (21) and (22), we have

$$
\begin{aligned}
\phi(0, \hat{y}_1) &= \phi^+(0, 1) + \phi_{\hat{y}}^+(0, 1)(\hat{y}_1 - 1) + e_1 \\
&= \phi^-(0, 0) + \phi_{\hat{y}}^-(0, 0)(\hat{y}_1) + e_2.
\end{aligned}
$$

The above equation implies

$$(23) \qquad (-1 + \hat{y}_1)\phi_{\hat{y}}^+(0, 1) - \hat{y}_1\phi_{\hat{y}}^-(0, 0) = \phi_1 - \phi_3 + e_2 - e_1.$$

Next, from the flux continuity and tangential continuity on the interface, we have

$$
(24) \qquad
\begin{aligned}
m_1\phi_{\hat{x}}^+ + m_2\phi_{\hat{y}}^+ &= \rho(m_1\phi_{\hat{x}}^- + m_2\phi_{\hat{y}}^-) \\
m_3\phi_{\hat{x}}^+ + m_4\phi_{\hat{y}}^+ &= m_3\phi_{\hat{x}}^- + m_4\phi_{\hat{y}}^-.
\end{aligned}
$$

By differentiating (21) and (22), and evaluating (22) at (1,0), we have

$$
(25) \qquad
\begin{cases}
\phi_{\hat{x}}^+(\hat{x}, \hat{y}) = \phi_{\hat{x}}^+(0, 1) + e_3 \\
\phi_{\hat{y}}^+(\hat{x}, \hat{y}) = \phi_{\hat{y}}^+(0, 1) + e_4 \\
\phi_{\hat{y}}^-(\hat{x}, \hat{y}) = \phi_{\hat{y}}^-(0, 0) + e_5 \\
\phi_{\hat{x}}^-(\hat{x}, \hat{y}) = \phi_{\hat{x}}^-(0, 0) + e_6,
\end{cases}
$$

here $e_i = o(h)$, $i = 3 \cdots 6$, and

$$(26) \qquad \phi_{\hat{x}}^-(0, 0) = \phi^-(1, 0) - \phi^-(0, 0) + e_2.$$

Now plugging (23), (25) and (26) into (24), the equation (24) can now be rewritten in a matrix form as following:

$$
(27)
\begin{aligned}
&\begin{bmatrix} m_1\hat{y}_1 & m_2(\hat{y}_1 + \rho(1 - \hat{y}_1)) \\ m_3\hat{y}_1 & m_4 \end{bmatrix}
\begin{bmatrix} \phi_{\hat{x}}^+(0, 1) \\ \phi_{\hat{x}}^+(0, 1) \end{bmatrix} \\
&= \begin{bmatrix} -\rho m_2 - \rho m_1\hat{y}_1 & \rho m_1\hat{y}_1 & \rho m_2 \\ -m_4 - m_3\hat{y}_1 & m_3\hat{y}_1 & m_4 \end{bmatrix}
\begin{bmatrix} \phi_1 \\ \phi_2 \\ \phi_3 \end{bmatrix} + \hat{y}_1 \begin{bmatrix} \tilde{e}_1 \\ \tilde{e}_2, \end{bmatrix}
\end{aligned}
$$

where $\tilde{e}_i = o(1)$, for $i = 1, 2$. Let $\delta_x^+ = (\phi_I^+)_{\hat{x}} - \phi_{\hat{x}}^+$, $\delta_y^+ = (\phi_I^+)_{\hat{y}} - \phi_{\hat{y}}^+$, $\delta_x^- = (\phi_I^-)_{\hat{x}} - \phi_{\hat{x}}^-$ and $\delta_y^- = (\phi_I^-)_{\hat{y}} - \phi_{\hat{y}}^-$. Recall that $a_1 = (\phi_I^+)_{\hat{x}}$, $a_2 = (\phi_I^+)_{\hat{y}}$, $b_1 = (\phi_I^-)_{\hat{x}}$, $b_2 = (\phi_I^-)_{\hat{y}}$, and

$$A = \begin{bmatrix} m_1\hat{y}_1 & m_2(\hat{y}_1 + \rho(1 - \hat{y}_1)) \\ m_3\hat{y}_1 & m_4 \end{bmatrix}$$

Subtracting (12) from (27) leads to the following equation

$$(28) \qquad A \begin{bmatrix} \delta_x^+(0, 1) \\ \delta_y^+(0, 1) \end{bmatrix} = \hat{y}_1 \begin{bmatrix} \tilde{e}_1 \\ \tilde{e}_2. \end{bmatrix}$$

By applying the lower bound of $det(A)$ in Remark 2.2 on the solution of the equation (28), we have

$$
\begin{aligned}
|\delta_x^+(0,1)| &= |\frac{\hat{y}_1(m_4\tilde{e}_1 - (\hat{y}_1 + \rho(1-\hat{y}_1))m_2\tilde{e}_2)}{det(A)}| \\
&< (|m_4\tilde{e}_1| + (\hat{y}_1 + \rho(1-\hat{y}_1))|m_2\tilde{e}_2|)\frac{h^2}{\min\{1,\rho\}} \\
&< c\frac{\max\{1,\rho\}}{\min\{1,\rho\}}h < c\cdot\max\{\rho,\frac{1}{\rho}\}h
\end{aligned}
$$

(29)

$$
\begin{aligned}
|\delta_y^+(0,1)| &= |\frac{\hat{y}_1(m_3\hat{y}_1\tilde{e}_1 + m_1\hat{y}_1\tilde{e}_2)}{det(A)}| \\
&< \hat{y}_1(|m_3\tilde{e}_1| + |m_1\tilde{e}_2|)\frac{h^2}{\min\{1,\rho\}}
\end{aligned}
$$

(30)

$$
< c\hat{y}_1\cdot\max\{\rho,\frac{1}{\rho}\}h
$$

Similarly, by subtracting (6) from (26) and subtracting (8) from (23), we have the following inequalities

(31)
$$
|\delta_x^-(0,0)| < ch^2
$$

$$
|\delta_y^-(0,0)| < |\frac{(-1+\hat{y}_1)}{\hat{y}_1}\delta_y^+(0,1)| + |\frac{e_1-e_2}{\hat{y}_1}|
$$

(32)
$$
< c\max\{\rho,\frac{1}{\rho}\}h + o(h^2).
$$

As a result of (25), (29), (30)-(32), the following error estimates hold

(33)
$$
\begin{aligned}
|(\phi_{\hat{x}}^+ - (\phi_I^+)_{\hat{x}})(\hat{x},\hat{y}))| &< |\phi_{\hat{x}}^+(\hat{x},\hat{y}) - \phi_{\hat{x}}^+(0,1)| + |(\phi_{\hat{x}}^+ - (\phi_I^+)_{\hat{x}})(0,1)| < c_1h \\
|(\phi_{\hat{y}}^+ - (\phi_I^+)_{\hat{y}})(\hat{x},\hat{y}))| &< |\phi_{\hat{y}}^+(\hat{x},\hat{y}) - \phi_{\hat{y}}^+(0,1)| + |(\phi_{\hat{y}}^+ - (\phi_I^+)_{\hat{y}})(0,1)| < c_2h,
\end{aligned}
$$

for $(\hat{x},\hat{y}) \in T^+ \setminus T^*$, and

(34)
$$
\begin{aligned}
|(\phi_{\hat{x}}^- - (\phi_I^-)_{\hat{x}})(\hat{x},\hat{y})| &\leq |\phi_{\hat{x}}^-(\hat{x},\hat{y}) - \phi_{\hat{x}}^-(0,0)| + |(\phi_{\hat{x}}^- - (\phi_I^-)_{\hat{x}})(0,0)| < c_3h \\
|(\phi_{\hat{y}}^- - (\phi_I^-)_{\hat{y}})(\hat{x},\hat{y})| &\leq |\phi_{\hat{y}}^-(\hat{x},\hat{y}) - \phi_{\hat{y}}^-(0,0)| + |(\phi_{\hat{y}}^- - (\phi_I^-)_{\hat{y}})(0,0)| < c_4h
\end{aligned}
$$

for $(\hat{x},\hat{y}) \in T^- \setminus T^*$, where $c_i = o\left(\max\{\rho,1/\rho\}\left\|D^2u\right\|_\infty\right)$, for $i = \cdots 4$.

Finally, for $(\hat{x},\hat{y}) \in T^*$, we have

$$
\nabla\phi(\hat{x},\hat{y}) - \nabla\phi_I(\hat{x},\hat{y}) = \nabla\phi(\bar{x},\bar{y}) - \nabla\phi_I(\bar{x},\bar{y}) + \delta_1 + \delta_2,
$$

for some $(\bar{x},\bar{y}) \in T^-$, where $\delta_1 = \nabla(\phi(\hat{x},\hat{y}) - \phi(\bar{x},\bar{y}))$ and $\delta_2 = \nabla(\phi_I^+ - \phi_I^-)(\hat{x},\hat{y})$. Since $\|\nabla(\phi - \phi_I)(\bar{x},\bar{y})\| < c_4h$ and $\|\delta_1\| < c_5h$, from (34) and Taylor formula, where c_5 depends on $\left\|D^2\phi\right\|_\infty$, we only need to estimate δ_2 to control the error $|\nabla\phi(\hat{x},\hat{y}) - \nabla\phi_I(\hat{x},\hat{y})|$.

Recall that from the flux continuity and tangential continuity, we have

$$
\begin{bmatrix} m_1 & m_2 \\ m_3 & m_4 \end{bmatrix} \begin{bmatrix} a_1 \\ a_2 \end{bmatrix} = \begin{bmatrix} \rho m_1 & \rho m_2 \\ m_3 & m_4 \end{bmatrix} \begin{bmatrix} b_1 \\ b_2 \end{bmatrix}.
$$

We can clearly see that,

$$
\begin{aligned}
\|\delta_2\| &= \|\nabla(\phi_I^- - \phi_I^+)(\hat{x},\hat{y})\| = \left\|\begin{bmatrix} a_1 - b_1 \\ a_2 - b_2 \end{bmatrix}\right\|
\end{aligned}
$$

(35)
$$
\leq \left\|\left(\begin{bmatrix} \rho m_1 & \rho m_2 \\ m_3 & m_4 \end{bmatrix}^{-1}\begin{bmatrix} m_1 & m_2 \\ m_3 & m_4 \end{bmatrix} - I\right)\right\|\left\|\begin{bmatrix} a_1 \\ a_2 \end{bmatrix}\right\|.
$$

From (33) and the assumption $\phi \in C^2(T)$, we have

$$(36) \qquad \left\| \begin{bmatrix} a_1 \\ a_2 \end{bmatrix} \right\| \leq \left\| \begin{bmatrix} a_1 \\ a_2 \end{bmatrix} - \begin{bmatrix} \phi_{\hat{x}}^+ \\ \phi_{\hat{y}}^+ \end{bmatrix} \right\| + \left\| \begin{bmatrix} \phi_{\hat{x}}^+ \\ \phi_{\hat{y}}^+ \end{bmatrix} \right\| < c_6,$$

for some constant c_6 depends on $\left\| D^2\phi \right\|_\infty$. Moreover, since

$$\left\| \begin{bmatrix} \rho m_1 & \rho m_2 \\ m_3 & m_4 \end{bmatrix}^{-1} \left(\begin{bmatrix} m_1 & m_2 \\ m_3 & m_4 \end{bmatrix} - I \right) \right\| \leq c_7 \left| \frac{1-\rho}{\rho h^{-2}} \right| \left\| \begin{bmatrix} m_1 m_4 & m_2 m_4 \\ -m_1 m_3 & -m_2 m_3 \end{bmatrix} \right\|$$

$$(37) \qquad\qquad\qquad\qquad\qquad\qquad \leq c_7 \left| \frac{1-\rho}{\rho} \right| \leq c_7 \max\{\frac{1}{\rho}, \rho\},$$

for some constant c_7, because m_1, m_2, m_3 and m_4 are $O(h^{-1})$. From (35), (36) and (37), we can conclude that

$$(38) \qquad \left\| \nabla\phi(\hat{x}, \hat{y}) - \nabla\phi_I(\hat{x}, \hat{y}) \right\|_\infty < c_8 \max\{\frac{1}{\rho}, \rho\} \text{ for } (\hat{x}, \hat{y}) \in T^*,$$

where the constant c_8 depends on $\left\| D^2\phi \right\|_\infty$. Finally, from (33), (34) and (38), we can conclude the inequality (19) holds. The inequality (20) can then be proved by following the same argument as shown in the Theorem 2.3 [27]. $\square$

With the help of the above theorem, we can easily obtain the traditional interpolation error estimation in the L^2-norm and H^1-norm.

Theorem 3.2. *The following interpolation error estimates hold. For function $\phi \in H^2(\Omega)$, if ϕ is a piecewise C^2 function on any interface element τ, for all $\tau \in \overset{\circ}{\Im}_h$, then there exist constants c_0 and c_1 such that*

$$(39) \qquad\qquad\qquad \left\| \phi - \phi_I \right\|_0 < c_0 h^2 \left\| \phi \right\|_2$$
$$(40) \qquad\qquad\qquad \left\| \phi - \phi_I \right\|_1 < c_1 h \left\| \phi \right\|_2,$$

where c_0 and c_1 are $O(\max\{1/\rho, \rho\})$.

Proof: We first prove inequality (39). It is clear that

$$\left\| \phi - \phi_I \right\|_0^2 = (\int_\Omega |\phi - \phi_I|^2 dx) = (\sum_{\tau \in \Im_h} \int_\tau |\phi - \phi_I|^2 dx)$$

$$\leq \sum_{\tau \in \Im_h} |\phi - \phi_I|_{\infty, \tau} \int_\tau |\phi - \phi_I| dx$$

$$\leq \max_{\tau \in \Im_h} \left\| \phi - \phi_I \right\|_{\infty, \tau} \sum_{\tau \in \Im_h} \left\| \phi - \phi_I \right\|_{0, \tau} (\int_\tau 1 dx)^{\frac{1}{2}}, \text{ by the Hölder inequality,}$$

$$\leq \max_{\tau \in \Im_h} \left\| \phi - \phi_I \right\|_{\infty, \tau} \left\| \phi - \phi_I \right\|_0 |\Omega|, \text{ by the Schwartz inequality.}$$

By theorem 3.1, this implies $\left\| \phi - \phi_I \right\|_0 \leq c h^2 \left\| \phi \right\|_2$, where c depends on $|\Omega|$ and $\max\{1/\rho, \rho\}$. Next, we show the estimation (40). It is well known that the inequality

$$(41) \qquad\qquad\qquad \left\| \phi - \phi_I \right\|_{1, \tau} \leq h \|\phi\|_{2, \tau}$$

holds, for elements $\tau \in \overset{\circ}{\Im}_h$ that do not intersect with interface. For an element $T \in \overset{\smile}{\Im}_h$ that intersects with the interface, we have

$$\int_T \nabla(\phi - \phi_I)\nabla(\phi - \phi_I) dx = \underbrace{\int_{T \backslash T^*} \nabla(\phi - \phi_I)\nabla(\phi - \phi_I) dx}_{I} + \underbrace{\int_{T^*} \nabla(\phi - \phi_I)\nabla(\phi - \phi_I) dx}_{II}.$$

By Theorem 3.1, we can clearly see that,

$$(I) \quad \leq \quad \|\nabla(\phi - \phi_I)\|_{\infty,T} \int_{T \setminus T^*} 1 \cdot \sqrt{\nabla(\phi - \phi_I)\nabla(\phi - \phi_I)} dx$$

$$(42) \qquad \leq \quad c_8 h|T|\|\nabla(\phi - \phi_I)\|_{0,T \setminus T^*} \|D^2\phi\|_{\infty,T},$$

and

$$(II) \quad \leq \quad \|\nabla(\phi - \phi_I)\|_{\infty,T^*} \int_{T^*} 1 \cdot \sqrt{\nabla(\phi - \phi_I)\nabla(\phi - \phi_I)} dx$$

$$(43) \qquad \leq \quad \|\nabla(\phi - \phi_I)\|_{\infty,T}\|\nabla(\phi - \phi_I)\|_{0,T^*}|T^*|.$$

Recall that Γ denotes the approximate line segment of the interface $\tilde{\Gamma}$ in an element. Let M be an arbitrary point in $\tilde{\Gamma}_T$ and $M^\perp$ be the orthogonal projection of M onto the line segment Γ. Based on the assumption (H_3), $\tilde{\Gamma}$ can be represented by a C^2 function in each element. It has been shown in [28] that there exists a constant $\tilde{c}$ such that $\|M - M^\perp\| < \tilde{c}h^2$. We can see clearly that,

$$(44) \qquad |T^*| = \int_0^{|\Gamma|} |\tilde{\Gamma}(s) - \Gamma(s)| ds \leq \tilde{c}h^3.$$

Plugging (44) into (43), and using Theorem 3.1, we can get

$$(45) \qquad (II) \leq \tilde{c}h|T| \|D^2\phi\|_{\infty,T} \|\nabla(\phi - \phi_I)\|_{0,T^*}.$$

Combining (42) and (45), we have

$$(46) \qquad \|\nabla(\phi - \phi_I)\|_{0,T} \leq \bar{c}h|T.| \|D^2\phi\|_{\infty,T}$$

Finally, from (41) and (46), we have

$$\|\phi - \phi_I\|_1^2 \quad \leq \quad \left(\sum_{\tau \in \Im_h} \|\nabla(\phi - \phi_I)\|_{0,\tau}^2 \right)^{1/2}$$

$$\leq \quad \bar{c}h \left(\sum_{\tau \in \Im_h} |\tau|^2 \right)^{1/2} \|\phi - \phi_I\|_1 \|D^2\phi\|_\infty.$$

here $\bar{c}$ depends on $\max\{\rho, c1/\rho\}$ and $|\Omega|$. As a result, the inequality (40) holds. □

Remark 3.3. *Let u and u_h^I denote the weak solution and the IFE solution of the interface problem (1) on the mesh $\Im_h$. The a-priori error estimate*

$$\|u - u_h^I\|_0 \leq ch^2 \|u\|_2 \quad and \quad \|u - u_h^I\|_\beta \leq ch \|u\|_2$$

follows directly from the interpolation error estimates in theorem 3.2 and the Galerkin orthogonal property.

To obtain posteriori error estimations, we follow Verfürth's work in [4]. By using the seminal inequalities, we know that

$$(47) \qquad \begin{cases} \|v\|_{0,\tau} \leq \gamma_1 \left\| \psi_\tau^{\frac{1}{2}} v \right\|_{0,\tau}, \\ \|\psi_\tau v\|_{1,\tau} \leq \gamma_2 h_\tau^{-1} \|v\|_{0,\tau}, \\ \|\sigma\|_{0,e} \leq \gamma_3 \left\| \psi_e^{\frac{1}{2}} \sigma \right\|_{0,e}, \\ \|\psi_e \sigma\|_{1,\tau} \leq \gamma_4 h_e^{-\frac{1}{2}} \|\sigma\|_{0,e}, \\ \|\psi_e \sigma\|_{0,\tau} \leq \gamma_5 h_e^{\frac{1}{2}} \|\sigma\|_{0,e}. \end{cases}$$

where v and σ are arbitrary polynomials of degree k, Verfürth has proposed an residual-based a-posteriori error indicator and shown that, for the finite element

solutions on an interface fitting grid, the effective constant between the local lower bound and the global upper bound is independent with the ratio $\rho = \beta^-/\beta^+$ of the flux jump across the interface. The analysis can be extended to higher order finite elements approximation as mentioned in [4]. In the following, we would like to show that with minor modification on the Verfürth's error indicator, the same estimates hold for the IFE solution.

Let $\varsigma = u - u_h^I$ and $\varsigma_\pi = I_\pi \varsigma$ be the quasi-interpolant of ς in $S_h(\Omega)$. By the theorem 2.1, there exist $\varsigma_\pi^I \in S_h^I(\Omega)$ such that $\varsigma_\pi^I(z) = \varsigma_\pi(z)$ for all $z \in \cup_{\tau \in \breve{\mathfrak{S}}_h} N_\tau$. By the orthogonality of the IFE solutions, we have

$$(48)\quad \|u - u_h^I\|_\beta^2 = \int_\Omega \beta \nabla(u - u_h^I)\nabla(u - u_h^I)$$

$$= \int_\Omega \beta \nabla(u - u_h^I) \left[\nabla(\varsigma - \varsigma_\pi) + \nabla \varsigma_\pi^I + \nabla(\varsigma_\pi - \varsigma_\pi^I) \right] dx$$

$$= \underbrace{\int_\Omega \beta \nabla(u - u_h^I) \nabla(\varsigma - \varsigma_\pi) dx}_{(III)} + \underbrace{\int_\Omega \beta \nabla(u - u_h^I) \nabla(\varsigma_\pi - \varsigma_\pi^I) dx}_{(IV)}.$$

First, we estimate (III) by the following Verfürth argument:

$$(III) = \sum_{\tau \in \mathfrak{S}_h} \int_\tau (-div(\beta \nabla u) + div \beta \nabla u_h)(\varsigma - \varsigma_\pi) dx$$

$$(49)\quad\quad - \sum_{e \in \mathcal{E}_h} \int_e [\beta \partial_h u_h]_e (\varsigma - \varsigma_\pi) ds$$

$$\leq \sum_{\tau \in \mathfrak{S}_h} \mu_\tau \left\| f + div \beta \nabla u_h^I \right\|_{0,\tau} \mu_\tau^{-1} \left\| \varsigma - \varsigma_\pi \right\|_{0,\tau}$$

$$+ \sum_{e \in \mathcal{E}_h} \mu_e^{\frac{1}{2}} \left\| [\beta \partial_n u_h^I]_e \right\|_{0,e} \mu_e^{-\frac{1}{2}} \left\| \varsigma - \varsigma_\pi \right\|_{0,e}$$

$$\leq \{ \sum_{\tau \in \mathfrak{S}_h} \mu_\tau^2 \left\| f + div \beta \nabla u_h^I \right\|_{0,\tau}^2 + \sum_{e \in \mathcal{E}_h} \mu_e \left\| [\beta \partial_n u_h^I] \right\|_{0,e}^2 \}^{\frac{1}{2}}$$

$$\{ \sum_{\tau \in \mathfrak{S}_h} \mu_\tau^{-2} \left\| \varsigma - \varsigma_\pi \right\|_{0,\tau}^2 + \sum_{e \in \mathcal{E}_h} \mu_e^{-1} \left\| \varsigma - \varsigma_\pi \right\|_{0,e}^2 \}^{\frac{1}{2}},$$

here, μ_τ and μ_e are parameters to be determined. It has been shown in [4] that the following inequalities

$$(50)\quad\quad \left\| \varsigma - \varsigma_\pi \right\|_{0,\tau} \leq c_1 h_\tau \beta_\tau^{-\frac{1}{2}} \left\| \varsigma \right\|_{\beta,\tilde{\omega}_\tau}$$

$$(51)\quad\quad \left\| \varsigma - \varsigma_\pi \right\|_{0,e} \leq c_2 h_e^{\frac{1}{2}} \beta_e^{-\frac{1}{2}} \left\| \varsigma \right\|_{\beta,\omega_e},$$

hold, where $\beta_e = \max_{\partial \tau_1 \cap \partial \tau_2 = e} \{\beta_{\tau_1}, \beta_{\tau_2}\}$. Combining the estimates (49)-(51), an estimation of (III) independent with the diffusive coefficients can be derived for the interface fitted grids by choosing $\mu_\tau = h_\tau \beta_\tau^{-\frac{1}{2}}$ and $\mu_e = h_e \beta_e^{-1}$ in (49). Therefore, by partition the mesh $\breve{\mathfrak{S}}_h$ into a regular interface fitted mesh and applying the zero flux jump condition on the interface Γ, we can easily show that the inequality (49) implies

$$(52)\quad (III) \leq c_{III} \{ \sum_{\tau \in \mathfrak{S}_h} \mu_\tau^2 \left\| f + div \beta \nabla u_h^I \right\|_{0,\tau}^2 + \sum_{e \in \mathcal{E}_h} \mu_e \left\| [\beta \partial_n u_h^I]_e \right\|_{0,e}^2 \}^{\frac{1}{2}} \left\| \varsigma \right\|_\beta,$$

where, for the element $\tau \in \breve{\Im}_h$ with $\tau = \tau^+ \cup \tau^-$,

$$\mu_\tau^2 \left\| f + div\beta \nabla u_h^I \right\|_{0,\tau}^2 = h_\tau^2 (\beta^+)^{-1} \left\| f + div\beta^+ \nabla u_h^I \right\|_{0,\tau^+}^2 + h_\tau^2 (\beta^-)^{-1} \left\| f + div\beta^- \nabla u_h^I \right\|_{0,\tau^-}^2,$$

for the edge $e \in \breve{\mathcal{E}}$ with $e = e^+ \cup e^-$, here $e^+ \subset \partial\tau^+ \setminus \Gamma$ and $e^- \subset \partial\tau^- \setminus \Gamma$,

$$\mu_e \left\| [\beta \partial_n u_h^I]_e \right\|_{0,e}^2 = h_e (\beta^+)^{-1} \left\| [\beta^+ \partial_n u_h^I]_{e^+} \right\|_{0,e^+}^2 + (h_e \beta^-)^{-1} \left\| [\beta^- \partial_n u_h^I]_{e^-} \right\|_{0,e^-}^2.$$

Next, we estimate (IV). By employing the usual homogenization arguments and the inequalities (18) in the remark 2.2, we have

$$
\begin{aligned}
\left\| \varsigma_\pi - \varsigma_\pi^I \right\|_{0,\tau} &\leq h_\tau \left\| \varsigma_\pi - \varsigma_\pi^I \right\|_{1,\tau} \leq c_1^I h_\tau \left\| \nabla \varsigma_\pi \right\|_{0,\tau} \\
(53) \qquad &\leq c_1^I h_\tau \left(\left\| \nabla(\varsigma_\pi - \varsigma) \right\|_{0,\tau} + \left\| \nabla \varsigma \right\|_{0,\tau} \right) \\
&\leq c_1^I \left(\left\| \varsigma_\pi - \varsigma \right\|_{0,\tau} + \beta^{-\frac{1}{2}} h_\tau \left\| \varsigma \right\|_{\beta,\tau} \right), \text{ by the inverse estimation,} \\
&\leq c_1^I h_\tau \beta^{-\frac{1}{2}} \left\| \varsigma \right\|_{\beta,\tilde{\omega}_\tau}, \text{ by (50),}
\end{aligned}
$$

where the constant $c_1^I = O(\max\{\rho, 1/\rho\})$. Similarly, by invoking the trace inequality, it can be shown that the following inequality holds

$$(54) \qquad\qquad \left\| \varsigma_\pi - \varsigma_\pi^I \right\|_{0,e} \leq c_2^I h_e^{\frac{1}{2}} \beta_e^{-\frac{1}{2}} \left\| \varsigma \right\|_{\beta,\omega_e},$$

where $c_2^I = O(\max\{\rho, \frac{1}{\rho}\})$.

By following the same arguments in (49) and (52) with (50) and (51) replaced by (53) and (54), we can conclude that the following estimate holds:

$$(55) \qquad (IV) \leq c_{IV} \Big\{ \sum_{\tau \in \Im_h} \mu_\tau^2 \left\| f + div\beta \nabla u_h^I \right\|_{0,\tau}^2 + \sum_{e \in \mathcal{E}_h} \mu_e \left\| [\beta \partial_n u_h^I]_e \right\|_{0,e}^2 \Big\}^{\frac{1}{2}} \left\| \varsigma \right\|_\beta,$$

where $C_{IV} = O(\max\{\rho, \frac{1}{\rho}\})$. The global a-posteriori error bound then follows from the estimates (48), (52) and (55), and is stated in the following theorem.

Theorem 3.4. *Let u and u_h^I be the solutions of the interface problem (1) in $H^1(\Omega)$ and $S_h^I(\Omega)$, respectively, and f_τ denote the piecewise constant of the L^2-projection of the function f on element τ. Let $\tau = \tau^+ \cup \tau^-$, for any element $\tau \in \breve{\Im}_h$, and $\partial^+\tau$ and $\partial^-\tau$ denote the sets of boundary line segments of the element τ that belong to the sets $\partial\tau^+ \setminus \Gamma$ and $\partial\tau^- \setminus \Gamma$, respectively. Assume that u has H^2 regularity on each element. There exist a constant c_p independent with the diffusive coefficients such that the following a-posteriori error bound holds.*

$$(56) \qquad\qquad \left\| u - u_h^I \right\|_\beta \leq c_p \Big\{ \sum_{\tau \in \Im_h} [\eta_\tau^2 + h_\tau^2 \beta_\tau^{-1} \left\| f - f_\tau \right\|_{0,\tau}] \Big\}^{\frac{1}{2}},$$

where

$$\eta_\tau = \left\{ h_\tau^2 \beta_\tau^{-1} \left\| f_h + div\beta_\tau \nabla u_h^I \right\|_{0,\tau}^2 + \frac{1}{2} \sum_{e \in \partial\tau} h_e \beta_\tau^{-1} \left\| \beta_\tau \left[\partial_{n_e} u_h^I \right] \right\|_{0,e}^2 \right\}^{\frac{1}{2}},$$

for $\tau \in \overset{\circ}{\Im}_h$, *and*

$$\eta_\tau = \left\{ \max\{\rho, \frac{1}{\rho}\} \left(\sum_{\tau' \in \{\tau^+, \tau^-\}} h_{\tau'}^2 \beta_{\tau'}^{-1} \left\| f_h + div\beta_{\tau'} \nabla u_h^I \right\|_{0,\tau'}^2 + \right. \right.$$

$$\left. \left. \frac{1}{2} \sum_{e' \in \{\partial^+\tau, \partial^-\tau\}} h_{e'} \beta_{e'}^{-1} \left\| \beta_{e'} \left[\partial_{n_{e'}} u_h^I \right] \right\|_{0,e'}^2 \right) \right\}^{\frac{1}{2}},$$

for $\tau \in \overset{\smile}{\Im}_h$, *here* $\beta_{e'} = \left\{ \begin{array}{ll} \beta^+ & \text{if } e' \in \partial^+\tau \\ \beta^- & \text{if } e' \in \partial^-\tau \end{array} \right.$.

4. Numerical examples

We now present some numerical results that support our theoretical results. Errors in the L^2 and H^1 norms of the IFE solutions to an interface problem will be given both on uniform triangular meshes and adaptively refined meshes. For simplicity, we solve the problem (1) in the rectangular domain $\Omega = (-1, 1) \times (-1, 1)$. The interface curve $\tilde{\Gamma}$ is a circle with radius $r_0 = 0.5$, which separates Ω into two sub-domains Ω^- and Ω^+ with

$$\Omega^- = \{(x, y) : x^2 + y^2 \leq r_0{}^2\}.$$

The exact solution considered here is as following,

(57) $$u(x, y) = \left\{ \begin{array}{ll} \dfrac{r^\alpha}{\beta^-}, & \text{if } r \leq r_0, \\ \dfrac{r^\alpha}{\beta^-} + (\dfrac{1}{\beta^-} - \dfrac{1}{\beta^+})r_0{}^\alpha & \text{otherwise}, \end{array} \right.$$

where $r = \sqrt{x^2 + y^2}$, $\alpha = 3$ and $\beta(x, y) = \left\{ \begin{array}{ll} \beta^-, & (x, y) \in \Omega^- \\ \beta^+, & (x, y) \in \Omega^+ \end{array} \right.$.

The interface problems demonstrated here have diffusive coefficients:

$$\beta_k(x, y) = \left\{ \begin{array}{ll} 1, & (x, y) \in \Omega^- \\ 10^k, & (x, y) \in \Omega^+ \end{array} \right. , k = 1 \cdots 3.$$

A sample uniform mesh and adaptive mesh over the domain Ω with the interface curve $\tilde{\Gamma}$, together with a typical IFE solution on the adaptive mesh for the case
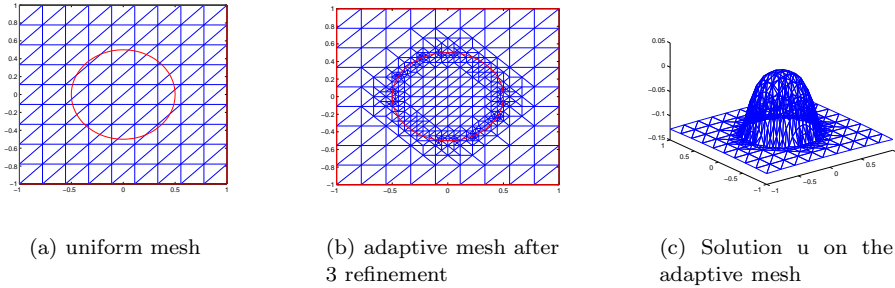

(a) uniform mesh

(b) adaptive mesh after 3 refinement

(c) Solution u on the adaptive mesh

FIGURE 3

h	$\frac{\beta_1^-}{\beta_1^+} = 10^{-1}$	$\frac{\beta_2^-}{\beta_2^+} = 10^{-2}$	$\frac{\beta_3^-}{\beta_3^+} = 10^{-3}$
$\frac{1}{8}$	3.689e-03	3.676e-03	4.164e-03
$\frac{1}{16}$	9.897e-04	9.998e-04	1.110e-03
$\frac{1}{32}$	2.700e-04	2.673e-04	3.370e-04
$\frac{1}{64}$	6.766e-05	6.318e-05	7.567e-05

TABLE 1. Errors for problems with various diffusive coefficients in the L^2 norm.

h	$\frac{\beta_1^-}{\beta_1^+} = 10^{-1}$	$\frac{\beta_2^-}{\beta_2^+} = 10^{-2}$	$\frac{\beta_3^-}{\beta_3^+} = 10^{-3}$
$\frac{1}{8}$	1.922e-01	4.677e-01	1.471e-00
$\frac{1}{16}$	8.314e-02	1.439e-01	4.390e-01
$\frac{1}{32}$	4.526e-02	8.726e-02	2.686e-01
$\frac{1}{64}$	2.222e-02	2.942e-02	8.394e-02

TABLE 2. Errors for problems with various diffusive coefficients in the energy norm.

$\beta^+ = 1000$ and $\beta^- = 1$, are shown in figure 3. Tables 1 and 2 contains the errors of the IFE solutions in the L^2 norm and the energy norm, respectively, on uniform meshes with grid size varies from $\frac{1}{8}$ to $\frac{1}{64}$. Using linear regression, we can see that the data in the table 1 obey

$$\left\| u - u_h^I \right\|_0 \approx 0.25 h^{1.97}, \; \left\| u - u_h^I \right\|_0 \approx 0.27 h^{2.00} \text{ and, } \left\| u - u_h^I \right\|_0 \approx 0.28 h^{1.96},$$

and the data in the table 2 obey

$$\left\| u - u_h^I \right\|_{\beta_1} \approx 1.71 h^{1.05}, \; \left\| u - u_h^I \right\|_{\beta_2} \approx 6.89 h^{1.30}, \text{ and } \left\| u - u_h^I \right\|_{\beta_3} \approx 6.75 h^{1.00}.$$

These results clearly indicate that the IFE solutions u_h^I converge to the exact solution u with convergence rates $O(h^2)$ and $O(h)$ in the L^2 norm and the energy norm, respectively, as mentioned in the remark 3.3.

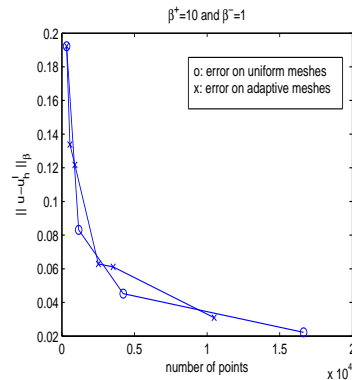| $|N_h|$	$\left\| u - u_h^I \right\|_\beta$	$(\sum_{\tau \in \Im_h} \eta_\tau^2)^{1/2}$
324	1.922e-01	4.117e-00
557	1.338e-01	2.316e-00
899	1.217e-01	1.756e-00
2516	6.281e-02	1.054e-00
3527	6.116e-02	7.515e-01
10482	3.097e-02	3.842e-01

FIGURE 4. The errors in the energy norm and the a-posteriori error bounds on adaptive meshes for the case $\beta^+ = 10$ and $\beta^- = 1$.

$|N_h|$	$\left\|u - u_h^I\right\|_\beta$	$(\sum_{\tau \in \Im_h} \eta_\tau^2)^{1/2}$
324	4.677e-01	1.136e+01
466	1.958e-01	1.538e+01
682	1.341e-01	2.280e-00
1507	5.495e-02	1.088e-00
4171	3.139e-02	5.201e-01
10243	2.188e-02	3.134e-01
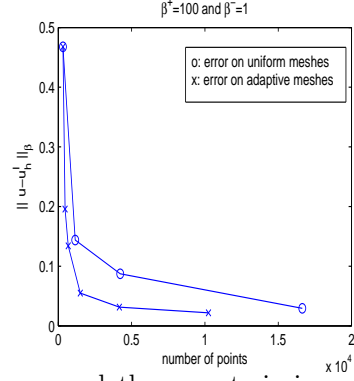
FIGURE 5. The errors in the energy norm and the a-posteriori error bounds on adaptive meshes for the case $\beta^+ = 100$ and $\beta^- = 1$.

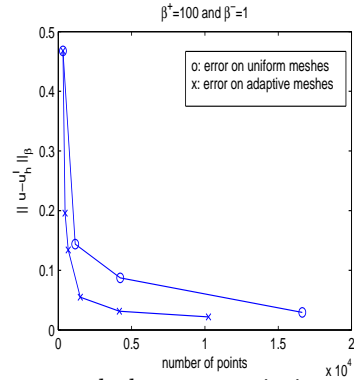| $|N_h|$	$\left\|u - u_h^I\right\|_\beta$	$(\sum_{\tau \in \Im_h} \eta_\tau^2)^{1/2}$
324	1.471e-00	1.592e+02
410	6.378e-01	1.659e+02
626	5.332e-01	8.339e-00
1066	2.057e-01	3.673e-00
1923	1.251e-01	1.572e-00
4021	4.105e-02	6.986e-01

FIGURE 6. The errors in the energy norm and the a-posteriori error bounds on adaptive meshes for the case $\beta^+ = 1000$ and $\beta^- = 1$.

Next, we compute the IFE solutions for the cases β_k, $k = 1 \cdots 3$ on adaptively refined meshes. To generate the adaptive meshes, the heuristic maximum marking strategy with threshold value 0.25 is employed. An element $\tau \in \Im_h$ will be marked for refinement if the associated error indicator value $\eta_\tau > 0.25 \max_{\tau' \in \Im_h} \eta_{\tau'}$. A regular mesh refinement scheme divides each marked triangle into 4 child triangles. Here, six levels of regular mesh refinement are performed on an initial 9×9 mesh. The tables on the left of the Figures 4, 5 and 6 contains the errors of the IFE solutions in the energy norms and the a-posteriori error bounds defined in the theorem 3.4 on the adaptive meshes. Comparisons of the errors on uniform meshes and adaptive meshes are shown on the right in each figure. From these figures, we can see that, on adaptive meshes, the accuracy of the IFE solutions is significantly increased and much less grid points are needed for the IFE solutions to reach a given error tolerance, when $\beta^+ \gg \beta^-$. In addition, the ratios of $(\sum_{\tau \in \Im_h} \eta_\tau^2)^{1/2}$ to $\left\|u - u_h^I\right\|_\beta$ tends to an order of 10 for all three cases when the number of mesh refinement is increased. This result suggests that the proposed a-posteriori error bound in theorem 3.4 is indeed independent with the diffusive coefficients.

5. Conclusions

In this paper, we have developed an adaptive mesh refinement technique for the non-conforming immersed finite element (IFE) method. The underlying triangulation and local mesh refinement does not need to fit the interface. The accuracy of the solution and its gradient is significant improved with the local adaptive mesh refinement. Some improved a-prior error estimate is also derived for the original non-conforming IFE method along with an a-posteriori error estimation needed for the adaptive mesh refinement technique.

Acknowledgments

References

[1] I. Babuška and W. C. Rheinboldt. Error estimates for adaptive finite element computations. *SIAM J. Numer. Anal.*, 15:736–754, 1978.

[2] R. E. Bank and A. Weiser. Some a posteriori error estimators for elliptic partial differential equations. *Math. Comp.*, 44:283–301, 1985.

[3] J. W. Barrett and C. M. Elliott. Fitted and unfitted finite element methods for elliptic equations with smooth interfaces. *IMA J. Numer. Anal.*, 7:283–300, 1987.

[4] C. Bernardi and R. Verfürth. Adaptive finite element methods for elliptic equations with non-smooth coefficients. *Numer. Math.*, 85:579–608, 2000.

[5] J. H. Bramble and J. T. King. A finite element method for interface problems in domains with smooth boundary and interfaces. *Advances in Comp. Math.*, 6:109–138, 1996.

[6] Z. Chen and J. Zou. Finite element methods and their convergence for elliptic and parabolic interface problems. *Numer. Math.*, 79:175–202, 1998.

[7] RW Clough and JL Toucher. Finite element stiffness matrices for analysis of plate bending. *Proceeding of Conference on Matrix Methods in Structural Mechanics, WPAFB, Ohio*, pages 515–545, 1965.

[8] A. Hansbo and P. Hansbo. An unfitted finite element method, based on nitsche's method, for elliptic interface problems. *Comp. Methods Appl. Mech. Engrg.*, 191:5537–5552, 2002.

[9] R. J. Leveque and Z. Li. The immersed interface method for elliptic equations with discontinuous coefficients and singular sources. *SIAM J Numer Anal*, 31:1019–1044, 1994.

[10] R. J. Leveque and Z. Li. Immersed interface method for stokes flow with elastic boundaries for source tension. *SIAM J Sci Comput*, 18:709–735, 1997.

[11] Z. Li and K. Ito. *The Immersed Interface Method-Numerical Solutions of PDEs Involving Interface and Irregular Domains*. SIAM Frontier Series in Applied Mathematics, FR33, 2006.

[12] Z. Li and J. Zou. Theoretical and numerical analysis on a thermo-elastic system with discontinuities. *J Comput Appl Math 91 (1998), 1-22.*, 91:1–22, 1998.

[13] R. H. Nochetto P. Morin and K. Siebert. Data oscillation and convergence of adaptive fem. *SIAM J. Numer. Anal.*, 38:466–488, 2000.

[14] A. Papastavrou and R. Verfürth. A posteriori error estimators for stationary convection-diffusion problems: a computational comparison. *Comput. Methods Appl. Mech. Engrg.*, 189:449–462, 2000.

[15] T. Lin R. Ewing, Z. Li and Y. Lin. The immersed finite volume element methods for the elliptic interface problems. *Math Comput Simul*, 50:63–76, 1999.

[16] M. C. Rivara. Algorithms for refining triangular grids suitable for adaptive and multigrid techniques. *Int. J. Numer. Methods Eng.*, 20:745–756, 1984.

[17] M. C. Rivara. Using longest-side bisection techniques for the automatic refinement of Delaunay triangulation. *Int. J. Numer. Methods Eng.*, 40:581–597, 1997.

[18] S. Osher T. Hou, Z. Li and H. Zhao. A hybrid method for moving interface problems with application to the hele-shaw flow. *J Comput Phys*, 134:234–252, 1997.

[19] T.Lin and J. Wang. An immersed finite element electric field solver for ion optics modeling. *Proceeding of AIAA Joint Propulsion Conference, Indianapolis, IN*, AIAA:2002–4263, 2002.

[20] T.Lin and J. Wang. An immersed finite element method for plasma particle simulation. *Proceeding of AIAA Aerospace Science Meeting, Reno, NV*, AIAA:2003–0842, 2003.

[21] R. Verfürth. A review of posteriori error estimation and adaptive mesh-refinement techniques. *Wiley and Teubner*, 1996.

[22] R. Verfürth. A posteriori error estimators for convection-diffusion equations. *Numer. Math.*, 80:641–663, 1998.

[23] A. Wiegmann and K. Bube. The immersed interface method for nonlinear differential equations with discontinuous coefficients and singular sources. *SIAM J Numer Anal 35 (1998), 177-200.*, 35:177–200, 1998.

[24] B. Li X. Yang and Z. Li. The immersed interface method for elasticity problems with interface. *Dynamics of Continuous, Discrete and Implusive Systems*, 10:783–808, 2003.

[25] Bo Li Yan Gong and Z. Li. Immersed interface finite element methods for elliptic interface problems with nonhomogeneous jump conditions. *SIAM J. Numer. Anal.*, 46:472–495, 2008.

[26] D. McTigue Z. Li and J. Heine. A numerical method for diffysive transport with moving boundaries and discontinuities material properties. *Int J Numer Anal Method Geomesh*, 21:653–672, 1997.

[27] T. Lin Z. Li and X.Wu. New cartesian grid methods for interface problems using finite element formulation. *Numer. Math.*, 96:61–98, 2003.

[28] Y. Lin Z. Li, T. Lin and R. C. Roger. An immersed finite element space and its approximation capability. *Numerical Methods of PDEs*, 20:338–367, 2004.

[29] O. C. Zienkiewicz and J. Z. Zhu. Adaptivity and mesh generation. *Int. J. Numer. Methods. Engrg.*, 32:783–810, 1991.

Department of Applied Mathematics, National Chiao-Tung University, 1001, Ta Hsueh Road, Hsinchu 300, Taiwan
   E-mail: `ctw@math.nctu.edu.tw`

Department of Mathematics, North Carolina State University, Raleigh, NC. 27695-8205, USA, and and School of Mathematical Sciences, Nanjing Normal University, Nanjing, China
   E-mail: `zhilin@math.ncsu.edu`

Center of mathematical modeling and Scientific computing, National Chiao-Tung University, 1001, Ta Hsueh Road, Hsinchu 300, Taiwan
   E-mail: `mclai@math.nctu.edu.tw`